Synthetic Wind Speed Scenarios Generation using Artificial Neural Networks for Probabilistic Analysis of Hybrid Energy Systems

Jun Chen
Dept. ECE, Oakland University
Rochester, MI 48309, USA
junchen@oakland.edu

Junhui Zhao
University of New Haven
West Haven, CT 06516, USA
jzhao@newhaven.edu

***Abstract*—Hybrid energy systems, which consist of multiple energy inputs and multiple energy outputs, have been proposed in literature to enable ever increasing penetration of clean energy. In order to properly design and analyze HES configuration, extensive data sets of renewable resources for the given location are required, whose availability may be limited due to insufficient historical measurement. This paper focuses on the methodology to generate synthetic scenarios of renewable resources, e.g., wind speed. Specifically, artificial neural networks (ANN) is utilized to characterize historical wind speed measurements and to generate synthetic scenarios, allowing Monte Carlo simulation of HES for probabilistic analysis. In addition, Fourier transformation is used to characterize the low frequency components in historical data, allowing the synthetic scenarios to preserve seasonal trend. Case study of probabilistic analysis is then performed on a particular HES configuration, which includes nuclear power plant, wind farm, battery storage, EV charging station, and desalination plant. Wind power availability and requirements on component ramping rate are then investigated.**

***Index Terms*—Wind power, synthetic scenarios, artificial neural networks, Fourier transformation, hybrid energy systems.**

I. Introduction

Hybrid energy systems (HES), which consist of multiple energy generations and utilization, have been proposed in literature [1]–[9] to enable higher level of renewable energy penetration. However, these prior analyses are performed based on historical measurements on renewable energy, whose availability is very limited for a given location. To address this limitation, this paper proposes a methodology to generate synthetic wind speed scenarios, which are shown to be statistically conformed to historical measurements, allowing probabilistic analysis of HES.

The synthetic wind speed scenarios generation has been studied in the literature to some extent. For example, [10] uses autoregressive moving average (ARMA) model to generate residues, and adds the synthetic residues to the historical data. Similarly, [11]–[15] use ARMA or AR model, together with sampled white noise, to generate scenarios. One of the assumptions of ARMA is that the underlying time series is normally distributed. To satisfy such assumption, the measurement data may need to be recast into Gaussian distribution before being used to train ARMA model. Reference [16] computes power spectrum density (PSD) through measurement data, predicts PSD based on future capacity, and generates sample waveform by inverse fast Fourier transformation of predicted PSD. Artificial neural networks (ANN) has been utilized for wind speed prediction in literature. For example, reference [17] decomposes the load data into low frequency part (i.e., deterministic seasonal trend part) and high frequency part. Both parts are used to train an ANN, one for each part. The two trained ANN models are then used to generate forecast. Reference [18] combines wavelet transform with ANN approach, while [19] uses Bayesian belief network to improve available load forecasting. Another approach to model the seasonal trend is to utilize Fourier transform to identify the low frequency components [20], [21]. Finally, some recent work [22], [23] use deep neural network to predict and synthesize renewable generation scenarios.

In this paper, we propose a new methodology to generate synthetic wind speed scenarios. Specifically, ANN is utilized to statistically characterize historical wind speed measurements and to generate synthetic scenarios, with 5 minutes resolution. Furthermore, Fourier transformation is used to characterize the low frequency components in historical data, allowing the synthetic scenarios to preserve seasonal trend. After training the model over historical data by finding optimal parameters, the combined model can then be used to generate synthetic scenarios. The generation process consists of generating noise term for each time step, evaluating ANN model to compute synthetic component for each time step, and finally adding the Fourier terms representing low frequency components (seasonal trends). By utilizing ANN, the challenging of data transformation into normal distribution, which is required by ARMA model [11], [12], is avoided. Furthermore, since the synthetic high frequency components have introduced sufficient variability compared to data set, the low frequency components, as identified by Fourier transformation, are adopted from historical data, i.e., no training and model evaluation are required and hence saving computation. Note

978-1-7281-9023-5/21/$31.00

that our approach differs from that of [17], which uses ANN to model both high frequency and low frequency components of electricity load data. Our approach is different from that of [23] which generates renewable power profile while wind speed, which has higher variation compared to power, is considered in our study. Furthermore, we demonstrate that a shallow network is sufficient to model the wind speed, hence saving computational time compared to deep learning approach. To validate the match between synthetic wind speed scenario and historical data set, statistical analysis (e.g., mean, variance, and empirical cumulative distribution function) as well as frequency analysis are performed. The generated synthetic wind speed scenarios will in turn be utilized to analyze a particular HES configuration, which includes nuclear power plant, wind farm, battery storage, EV charging station, and desalination plant. Wind power availability and requirements on component ramping rate are then investigated.

II. Synthetic Wind Speed Scenarios based on ANN

We start this section by giving a brief introduction of artificial neural networks (ANN), which is later employed to capture the nonlinear autocorrelation function of wind speed. Readers can refer to [24], [25] for more details.

A. Artificial Neural Network

ANN is a popular machine learning technique for modeling complex nonlinear relationship between inputs and outputs [24]. Denote x as the input to a neuron i, its output y is computed according to the following activation function $y = f_{ac}(w_i^T x + b_i)$ where the weights w_i and bias b_i are model parameters to be identified from data through training process. Denote the number of input neurons as p, and the number of output neurons as l, to train a neural network requires training data consisting of input $X_{p\times N}$ and output $Y_{l\times N}$, where N is the number of samples. Given a uni-variate time series $\mathbf{x} = x_1, x_2, \ldots, x_L$, in order to capture the autocorrelation, one can construct the following training data with $N = L - p$ and $l = 1$, where p can be chosen as the lag of autocorrelation,

$$X_{p\times(L-p)} = \begin{bmatrix} x_1 & x_2 & \cdots & x_{L-p} \\ x_2 & x_3 & \cdots & x_{L-p+1} \\ \vdots & \vdots & & \vdots \\ x_p & x_{p+1} & \cdots & x_{L-1} \end{bmatrix} \tag{1}$$

$$Y_{1\times(L-p)} = \begin{bmatrix} x_{p+1} & x_{p+2} & \cdots & x_L \end{bmatrix} \tag{2}$$

B. Historical Data Set and ANN Training

To capture the autocorrelation of wind speed, a one-year historical wind speed data set[1] is utilized to train ANN, which is a discrete time uni-variate time series with 5 minutes interval. To train ANN, this wind speed data set, denoted as $\mathbf{x}_w = x_1, x_2, \ldots, x_L$, where $L = 105,120$, can be transformed into training input $X_{p\times(L-p)}$ and output Y_{L-p} according to (1) and (2). The number of input neurons, p, which captures the lag of the autocorrelation of wind speed, can be selected based on the partial autocorrelation function of wind speed. In this paper, a lag of 3 is sufficient to capture the autocorrelation of the data. Algorithm 1 summarizes the procedure for data preprocessing and model training for synthetic wind speed scenarios generation.

[1]Downloaded from the Eastern Wind data set maintained by NREL (National Renewable Energy Laboratory) at http://www.nrel.gov/electricity/transmission/eastern_wind_dataset.html on November 21, 2019.

Algorithm 1 Algorithm to train ANN for generating synthetic wind speed scenarios

procedure SYNTHETIC_WIND_TRAIN($\mathbf{x}_w$)
  Compute empirical partial autocorrelation `pacf` of $\mathbf{x}_w$;
  $p \leftarrow \arg\max_k |\texttt{pacf}(k)| > 0.05$;
  Construct $X_{p\times(L-p)}$ and Y_{L-p} according to (1)–(2);
  Instantiate `net` $\leftarrow$ an ANN with p inputs and 1 output;
  Train `net` on $X_{p\times(L-p)}$ and Y_{L-p};
  return `net`
end procedure

C. Synthetic Scenarios Generation Using Trained ANN

Once the ANN is trained, it can be utilized to generate synthetic wind speed scenarios by recursively evaluating it over the past p data point in the synthetic time series. Denote the synthetic wind speed data as $\hat{\mathbf{x}}_w$, and assume the first p elements (i.e., $\hat{x}_1, \ldots, \hat{x}_p$) are given (whose generation will be detailed shortly). Then for $k = p+1, \ldots, L$,

$$\hat{x}_k = \texttt{net}(\begin{bmatrix} \hat{x}_{k-p} & \cdots & \hat{x}_{k-1} \end{bmatrix}^T) + \sigma_k \tag{3}$$

where σ_k denotes a random noise to avoid degeneration.

Remark 1: The purpose of adding σ_k in (3) is to provide sufficient excitation in the recursive generation process. Without this excitation, in practice, the synthesized time series may converge to a constant value as the process degenerates. Note that σ_k can be sampled either through a pre-selected distribution, or through the error vector between the trained ANN (denoted as `net`) and Y_{L-p}. Denote the error vector $\mathbf{e}$ with length $L - p$, then for $k = 1, \ldots, L-p$,

$$e_k = \texttt{net}(\begin{bmatrix} x_k & \cdots & x_{k+p-1} \end{bmatrix}^T) - x_{k+p}. \tag{4}$$

Algorithm 2 summarizes the procedure that generates N synthetic wind speed scenarios based on trained ANN `net`.

D. Numerical Results and Discussion

This section presents numerical results of the procedures presented in Algorithms 1 and 2. Fig. 1 compares 7 days of the synthetic wind speed and that of the historical data set. As can be seen, the synthetic scenario presents completely different time profile compared to that of the data set, which can be utilized to perform probabilistic analysis of wind power generation.

Despite the completely different time profiles, the synthetic wind speed and historical data set actually possess similar statistical characteristics. Several key statistics of the synthetic scenarios and data set are summarized in Table I, showing

Algorithm 2 Algorithm to generate synthetic wind speed scenarios

procedure SYNTHETIC_WIND_GENERATE(net, N)
  $\mathbf{e} \leftarrow \texttt{net}(X_{p\times(L-p)}) - Y_{L-p}$;
  for $n = 1, \ldots, N$ **do**
    Obtain $\mathbf{e}_n$ by sampling from elements of $\mathbf{e}$ for L times;
    for $k = 1, \ldots, p$ **do**
      $\hat{\mathbf{x}}_n(k) \leftarrow \mathbf{x}_w(k) + \mathbf{e}_n(k)$
    end for
    for $k = p+1, \ldots, L$ **do**
      $d \leftarrow \left[\begin{array}{ccc} \hat{\mathbf{x}}_n(k-p) & \cdots & \hat{\mathbf{x}}_n(k-1) \end{array} \right]^T$
      $\hat{\mathbf{x}}_n(k) \leftarrow \texttt{net}(d) + \mathbf{e}_n(k)$
    end for
  end for
  $\hat{\mathbf{x}} \leftarrow \left[\begin{array}{ccc} \hat{\mathbf{x}}_1 & \cdots \hat{\mathbf{x}}_N \end{array} \right]$
  return $\hat{\mathbf{x}}$
end procedure

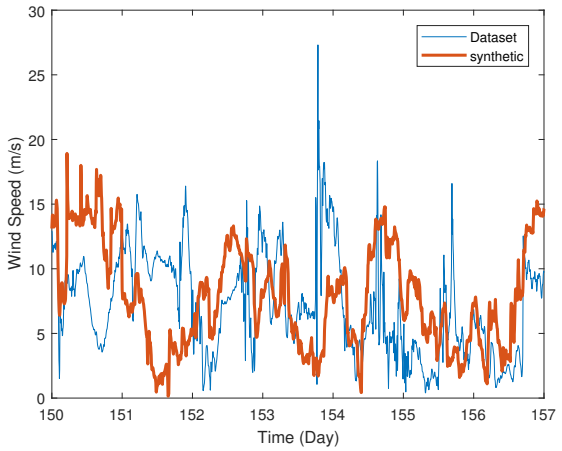

Fig. 1. Synthetic wind speed versus historical data set for a selected period of 7 days.

Stats	Data set	Synthetic
Max	30.60	30.82
95 percentile	14.67	14.38
Mean	8.16	8.16
Median	8.09	8.29
Standard deviation	3.91	3.78
5 percentile	2.04	1.97
Min	0.02	0.01

TABLE I
COMPARISON OF KEY STATISTICS OF SYNTHETIC SCENARIOS AND HISTORICAL DATA SET.

good alignment between the synthetic scenarios and data set. Furthermore, Fig. 2 plots the empirical cumulative density function (CDF) between synthetic wind speed and historical data set, where satisfactory statistical conformance can also be found, despite of the completely different time profile as shown in Fig. 1. Furthermore, Table II compares the power density of the synthetic scenarios and historical data set, again showing good alignment between the two.

Despite the good statistical conformance discussed above, the proposed procedure does present one drawback. As can be

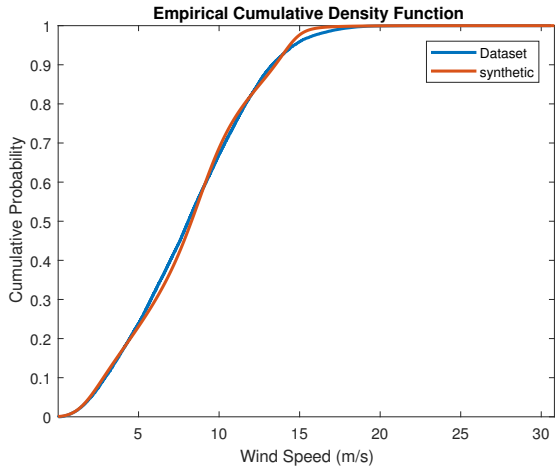

Fig. 2. Empirical cumulative density function for synthetic wind speed versus data set.

Period	Data set (dB/Hz)	Synthetic (dB/Hz)
$\geq$ 3 months	75.53	72.47
$\geq$ 1 month	62.18	57.12
$\geq$ 1 week	59.20	60.24
$\geq$ 1 day	55.27	55.54
$\geq$ 1 hour	33.06	33.45
$\geq$ 0.5 hour	21.70	22.30
$<$ 0.5 hour	10.50	9.92

TABLE II
COMPARISON OF POWER DENSITY OF SYNTHETIC SCENARIOS AND HISTORICAL DATA SET.

noticed from Algorithm 1 and 2, the timing information (e.g., time of the year) is not taken into account when generating the synthetic scenarios. The lack of such information does not impact the overall statistical distribution; however, it does impact the monthly (or even weekly) trend that the historical data set presents. In particular, Fig. 3 compares the monthly average wind speed of synthetic scenarios and historical data set. It is clear that the synthetic wind speed does not preserve the seasonal trend that exists in the data set. Note that this may not be an issue for analysis that does not depend on seasonal trend, but for analysis that does, such limitation can be problematic. To overcome this, in the following section, we proposed a revised procedure that removes the low frequency components from the training and generation process.

III. SYNTHETIC WIND SPEED SCENARIOS GENERATION PRESERVING SEASONAL TREND

In this section, we propose a revised procedure that removes the low frequency components from the training and generation process. In other words, the ANN is only used to generate synthetic high frequency components, while the low frequency components are taken from the historical data set. We start this section by giving a brief introduction of discrete Fourier transform (DFT) and fast Fourier transform (FFT). More details can be found in [26].

A. Discrete Fourier Transform

Given a time series $\mathbf{x} = x_0, x_1, \ldots, x_{L-1}$, the DFT transforms it into another sequence $\bar{\mathbf{x}} = \bar{x}_0, \bar{x}_1, \ldots, \bar{x}_{L-1}$ defined

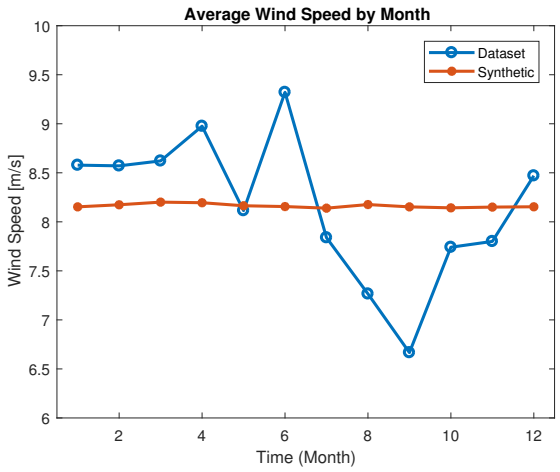

Fig. 3. Monthly trend of the historical data set and synthetic scenario.

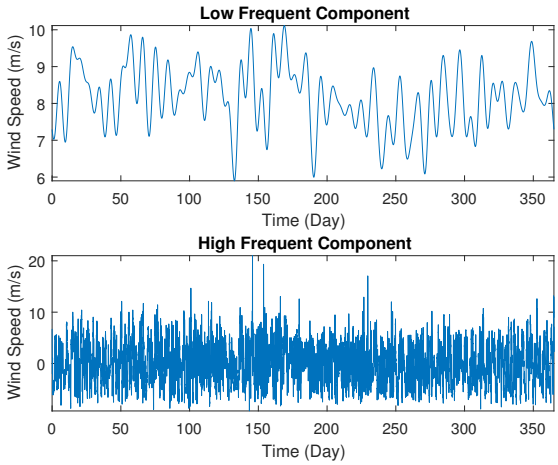

Fig. 4. Low frequency and high frequency components of historical wind speed data set.

by

$$\bar{x}_k = \sum_{n=0}^{L-1} x_n \left[\cos\left(\frac{2\pi}{L}kn\right) - i\sin\left(\frac{2\pi}{L}kn\right)\right].$$

Denote this transform by $\mathcal{F}$, we have $\bar{\mathbf{x}} = \mathcal{F}(\mathbf{x})$. The inverse discrete Fourier transform, denoted as $\mathcal{F}^{-1}$, transforms $\bar{\mathbf{x}}$ back to $\mathbf{x}$, i.e., $\mathbf{x} = \mathcal{F}^{-1}(\bar{\mathbf{x}})$, and can be computed according to

$$x_k = \frac{1}{N}\sum_{n=0}^{L-1} \bar{x}_n \left[\cos\left(\frac{2\pi}{L}kn\right) + i\sin\left(\frac{2\pi}{L}kn\right)\right].$$

It is easy to see that $\bar{x}_n$ denotes the amplitude of the component at period of $\frac{L}{n}T_s$ (or equivalently at frequency of $\frac{n}{LT_s}$), where T_s is the sampling interval of the time series $\mathbf{x}$.

B. Revised Algorithm Preserving Seasonal Trend

According to Section III-A, given a wind speed time series $\mathbf{x}_w$ with length L, its Fouries transformation can be computed by $\bar{\mathbf{x}}_w = \mathcal{F}(\mathbf{x}_w)$ such that the nth element $\bar{x}_n$ of $\bar{\mathbf{x}}_w$ indicates the amplitude of the component at frequency $\frac{n}{LT_s}$. Given q such that $\frac{q}{LT_s}$ (approximately) equals to a cutoff frequency f_c, and

$$\bar{\mathbf{x}}_L = \left[\ \bar{x}_1, \ldots \bar{x}_q, 0, \ldots, 0\ \right] \quad (5)$$

$$\bar{\mathbf{x}}_H = \left[\ \bar{0}, \ldots \bar{0}, \bar{x}_{q+1}, \ldots, \bar{x}_L\ \right], \quad (6)$$

then the high frequency components $\mathbf{x}_H$ and low frequency components $\mathbf{x}_L$ of $\mathbf{x}_w$ can be computed by

$$\mathbf{x}_L = \mathcal{F}^{-1}(\bar{\mathbf{x}}_L) \quad (7)$$

$$\mathbf{x}_H = \mathcal{F}^{-1}(\bar{\mathbf{x}}_H). \quad (8)$$

Fig. 4 shows the low frequency and high frequency components of the historical wind speed data set, where $f_c = 1.649$ μHz, corresponding to a period of one week.

Once $\mathbf{x}_H$ and $\mathbf{x}_L$ are obtained, an ANN `net_h` can be trained over $\mathbf{x}_H$ utilized Algorithm 1, which can then be used to generate synthetic high frequency components using Algorithm 2. The synthetic high frequent components are then shifted by $\mathbf{x}_L$ to obtain the synthetic wind speed. This procedure is summarized in Algorithm 3 and 4.

Algorithm 3 Algorithm to train ANN using only high frequency components

procedure SYNTHETIC_WIND_HIGH_TRAIN($\mathbf{x}_w$, f_c)
  $\bar{\mathbf{x}}_w \leftarrow \mathcal{F}(\mathbf{x}_w)$; $\bar{\mathbf{x}}_H \leftarrow \bar{\mathbf{x}}_w$; $\bar{\mathbf{x}}_L \leftarrow \bar{\mathbf{x}}_w$;
  $q \leftarrow \lceil f_c L T_s \rceil$;
  for $k = 1, \ldots, q$ **do**
    $\bar{\mathbf{x}}_H(k) \leftarrow 0$
  end for
  for $k = q+1, \ldots, L$ **do**
    $\bar{\mathbf{x}}_L(k) \leftarrow 0$
  end for
  $\mathbf{x}_L \leftarrow \mathcal{F}^{-1}(\bar{\mathbf{x}}_L)$; $\mathbf{x}_H \leftarrow \mathcal{F}^{-1}(\bar{\mathbf{x}}_H)$
  `net_h` $\leftarrow$ SYNTHETIC_WIND_TRAIN($\mathbf{x}_H$)
  return `net_h`, $\mathbf{x}_L$
end procedure

C. Numerical Results and Discussion

Fig. 5 and 6 summarize the results using Algorithms 3 and 4 with $f_c = 1.649$ μHz. In particular, Fig. 5 plots the synthetic wind speed versus historical data set for a selected period of 7 days, where only the high frequency components are synthetic. Fig. 6 compares the monthly average wind speed of synthetic scenarios and historical data set, which shows

Algorithm 4 Revised algorithm to generate synthetic wind speed scenarios

procedure SYNTHETIC_WIND_HIGH_GENERATE(`net_h`, $\mathbf{x}_L$, N)
  for $n = 1, \ldots, N$ **do**
    $\hat{\mathbf{x}}_1 \leftarrow$ SYNTHETIC_WIND_GENERATE(`net_h`, 1)
    $\hat{\mathbf{x}}_1 \leftarrow \mathbf{x}_L + \hat{\mathbf{x}}_1$
  end for
  $\hat{\mathbf{x}} \leftarrow \left[\ \hat{\mathbf{x}}_1 \quad \cdots \hat{\mathbf{x}}_N\ \right]$
  return $\hat{\mathbf{x}}$
end procedure

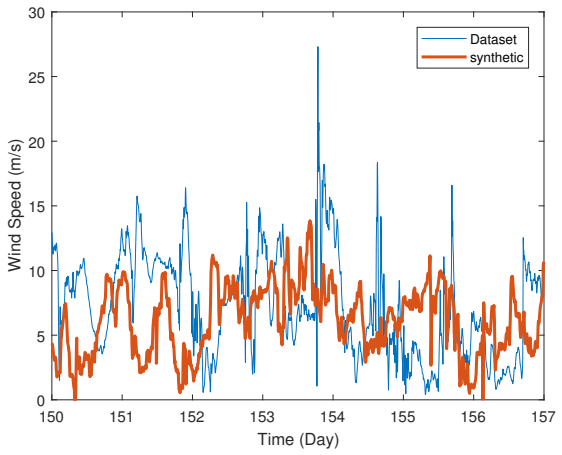

Fig. 5. Synthetic wind speed versus historical data set for a selected period of 7 days, with only high frequency components being synthetic.

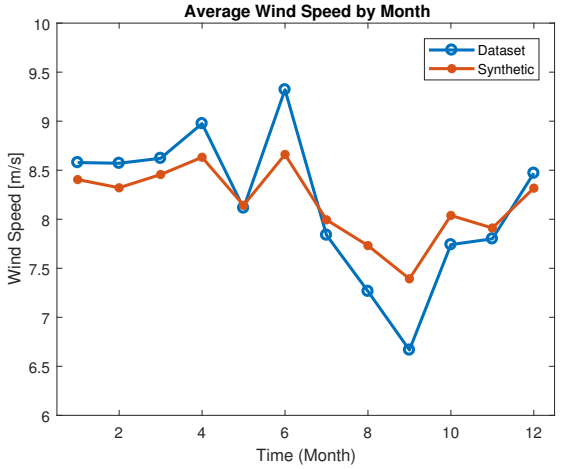

Fig. 6. Monthly trend of the historical data set and synthetic scenarios, with only high frequency components being synthetic.

that the synthetic wind speed can preserve the monthly trend exhibited in the data set. Therefore, the proposed algorithms in this section can generate a set of wind speed profiles that possess rich variation in terms of time series, while at the same time preserves the seasonal trends exhibited in the data set.

Finally, Table III analyzes the impact of f_c in Algorithm 3 and 4, by sweeping f_c through different values. Specifically, the root mean square error (RMSE) between synthetic wind speed and historical data set is used to quantified the impact of f_c. As can be seen, as f_c increase, higher frequency components are removed from the training and evaluation process, leaving less components being synthetic. Consequently, the synthetic wind speed presents a more similar time profile compared to data set, resulting a smaller RMSE, as demonstrated in Table III.

Remark 2: Note that RMSE can also be viewed as a metric to quantify the variation of the synthetic scenarios. Since the goal here is to generate a time profile that is *different* from historical data set, the larger RMSE the better. However, as illustrated in Fig. 3 and 6, the larger RMSE might also reduce the seasonal trend, which can be important for some studies

f_c (μHz)	Period	RMSE (m/s)
0.0634	3 months	5.3503
0.3805	1 month	5.2525
1.649	1 week	4.8264
11.57	1 day	3.5168
277.8	1 hour	2.5016

TABLE III
ROOT MEAN SQUARE ERROR BETWEEN SYNTHETIC WIND SPEED AND HISTORICAL DATA SET.

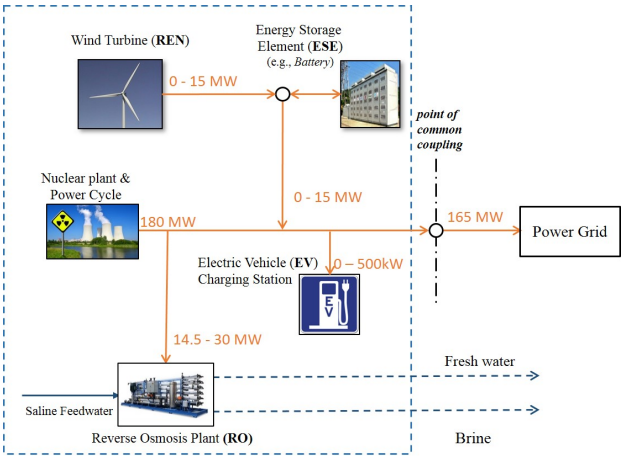

Fig. 7. Topology of the hybrid energy system configuration under study.

such as economic analysis where the electrical price presents strong seasonal trend.

IV. Probabilistic Analysis of HES

This section applies the previous results to probabilistic analysis of a specific HES configuration, whose topology is shown within the dotted line in Fig. 7 and includes:

- a baseline electricity generation with 180 MW capacity, consisting of a small modular reactor (SMR), a steam generator, a power cycle converting steam into electricity,
- a series of wind turbines as renewable power generation source with total capacity of 15 MW,
- an energy storage element (ESE) used for power smoothing of the electricity generated by wind turbines,
- a reverse osmosis (RO) plant converting saline water to potable water by consuming electricity between 14.5 MW and 30 MW,
- an electric vehicle (EV) charging station consuming electricity between 0 and 500 kW,
- electric grid connected to HES at a point of common coupling and consuming 165 MW electricity from HES.

The HES is operated in such a way that it supplies 165 MW of electricity to the power grid, and the volatility from wind farm and EV charging station is absorbed by ESE and RO plant. An optimization framework to flexibly operate RO plant is discussed in [9], which relies on historical measurements of wind speed data. To perform probabilistic analysis, 3,000 synthetic wind speed profiles are generated using Algorithm 3 and 4 with $f_c = 1.649$ μHz.

Among these 3,000 simulation, the wind farm power has a mean of 4.264 MW and standard deviation of 0.129 MW.

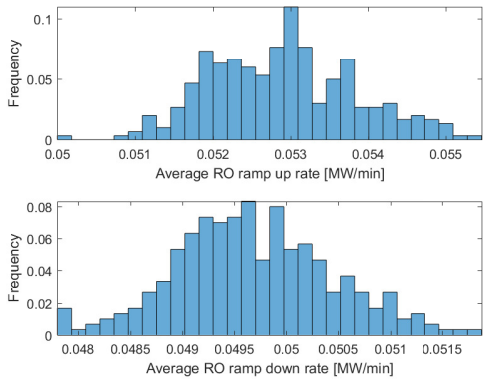

Fig. 8. Histogram of average ramp-up/-down rates for RO chemical plant.

Finally, Fig. 8 plots the histogram of the maximum RO ramp-up and ramp-down rate required to absorb the volatility. Note that the effect of ESE has been considered in these plots. These results can be helpful when considering the resiliency of the HES to accommodate both the average and worst case scenarios.

V. Conclusion

This paper focuses on synthetic scenarios generation for wind speed. In particular, artificial neural networks is utilized to characterize historical wind speed measurements and to generate synthetic scenarios. In addition, Fourier transformation is used to characterize the low frequency components in historical data set, allowing the synthetic scenarios to preserve seasonal trend. The synthetic wind speed scenarios are then utilized to perform probabilistic analysis of a hybrid energy systems, which includes nuclear power plant, wind farm, battery storage, EV charging station, and desalination chemical plant. Wind power availability and requirements on component ramping rate are then investigated. Future work includes parallel computing to allow fast scenarios generation and HES simulation. Designing the optimal ANN architecture is another future direction.

Acknowledgement

This project is supported in part by the faculty startup fund from School of Engineering and Computer Science at Oakland University.

References

[1] H. E. Garcia, A. Mohanty, W. Lin, and R. Cherry, "Dynamic analysis of hybrid energy systems under flexible operation and variable renewable generation –- part i: Dynamic performance analysis," *Energy*, vol. 52, pp. 1–16, 2013.

[2] ——, "Dynamic analysis of hybrid energy systems under flexible operation and variable renewable generation -– part ii: Dynamic cost analysis," *Energy*, vol. 52, pp. 17–26, 2013.

[3] M. Ippolito, M. Di Silvestre, E. R. Sanseverino, G. Zizzo, and G. Graditi, "Multi-objective optimized management of electrical energy storage systems in an islanded network with renewable energy sources under different design scenarios," *Energy*, vol. 64, pp. 648–662, 2014.

[4] J. S. Kim, J. Chen, and H. E. Garcia, "Modeling, control, and dynamic performance analysis of a reverse osmosis desalination plant integrated within hybrid energy systems," *Energy*, vol. 112, pp. 52–66, 2016.

[5] H. E. Garcia, J. Chen, J. S. Kim, R. B. Vilim, W. R. Binder, S. M. B. Sitton, R. D. Boardman, M. G. McKellar, and C. J. Paredis, "Dynamic performance analysis of two regional nuclear hybrid energy systems," *Energy*, vol. 107, pp. 234–258, 2016.

[6] M. L. Di Silvestre, G. Graditi, and E. R. Sanseverino, "A generalized framework for optimal sizing of distributed energy resources in micro-grids using an indicator-based swarm approach," *IEEE Transactions on Industrial Informatics*, vol. 10, no. 1, pp. 152–162, 2014.

[7] B. Zhu, H. Tazvinga, and X. Xia, "Switched model predictive control for energy dispatching of a photovoltaic-diesel-battery hybrid power system," *IEEE Trans. Control Syst. Tech.*, vol. 23, no. 3, pp. 1229–1236, May 2015.

[8] G. Graditi, M. L. Di Silvestre, R. Gallea, and E. Riva Sanseverino, "Heuristic-based shiftable loads optimal management in smart micro-grids," *IEEE Transactions on Industrial Informatics*, vol. 11, no. 1, pp. 271–280, 2015.

[9] J. Chen and H. E. Garcia, "Economic optimization of operations for hybrid energy systems under variable markets," *Applied Energy*, vol. 177, pp. 11–24, 2016.

[10] P. Meibom, R. Barth, B. Hasche, H. Brand, C. Weber, and M. O'Malley, "Stochastic optimization model to study the operational impacts of high wind penetrations in ireland," *IEEE Trans. Power Syst.*, vol. 26, no. 3, pp. 1367–1379, 2011.

[11] J. Chen and C. Rabiti, "Synthetic wind speed scenarios generation for probabilistic analysis of hybrid energy systems," *Energy*, vol. 120, pp. 507–517, 2017.

[12] J. Chen, J. S. Kim, and C. Rabiti, "Probabilistic analysis of hybrid energy systems using synthetic renewable and load data," in *Prof. 2017 American Control Conference*, Seattle, WA, May, 2017, pp. 4723–4728.

[13] J. M. Morales, R. Minguez, and A. J. Conejo, "A methodology to generate statistically dependent wind speed scenarios," *Applied Energy*, vol. 87, no. 3, pp. 843–855, 2010.

[14] A. Papavasiliou, S. S. Oren, and R. P. O'Neill, "Reserve requirements for wind power integration: A scenario-based stochastic programming framework," *IEEE Trans. Power Syst.*, vol. 26, no. 4, pp. 2197–2206, 2011.

[15] X.-Y. Ma, Y.-Z. Sun, and H.-L. Fang, "Scenario generation of wind power based on statistical uncertainty and variability," *IEEE Trans. Sustainable Energy*, vol. 4, no. 4, pp. 894–904, 2013.

[16] D. Lee and R. Baldick, "Future wind power scenario synthesis through power spectral density analysis," *IEEE Trans. Smart Grid*, vol. 5, no. 1, pp. 490–500, 2014.

[17] E. Gonzalez-Romera, M. A. Jaramillo-Moran, and D. Carmona-Fernandez, "Monthly electric energy demand forecasting based on trend extraction," *IEEE Trans. Power Syst.*, vol. 21, no. 4, pp. 1946–1953, 2006.

[18] N. Amjady and F. Keynia, "Short-term load forecasting of power systems by combination of wavelet transform and neuro-evolutionary algorithm," *Energy*, vol. 34, no. 1, pp. 46–57, 2009.

[19] N. Steckler, A. Florita, J. Zhang, and B. Hodge, "Analysis and synthesis of load forecasting data for renewable integration studies," in *Proc. 12th International Workshop on Large-Scale Integration of Wind Power into Power Systems*, London, England, Oct. 22-24, 2013.

[20] L. J. Soares and M. C. Medeiros, "Modeling and forecasting short-term electricity load: A comparison of methods with an application to brazilian data," *International Journal of Forecasting*, vol. 24, no. 4, pp. 630–644, 2008.

[21] K. K. Sumer, O. Goktas, and A. Hepsag, "The application of seasonal latent variable in forecasting electricity demand as an alternative method," *Energy policy*, vol. 37, no. 4, pp. 1317–1322, 2009.

[22] K. Chen, K. Chen, Q. Wang, Z. He, J. Hu, and J. He, "Short-term load forecasting with deep residual networks," *IEEE Transactions on Smart Grid*, vol. 10, no. 4, pp. 3943–3952, 2018.

[23] Y. Chen, Y. Wang, D. Kirschen, and B. Zhang, "Model-free renewable scenario generation using generative adversarial networks," *IEEE Transactions on Power Systems*, vol. 33, no. 3, pp. 3265–3275, 2018.

[24] C. M. Bishop *et al.*, *Neural networks for pattern recognition*. Oxford university press, 1995.

[25] M. Mohri, A. Rostamizadeh, and A. Talwalkar, *Foundations of machine learning*. MIT press, 2018.

[26] A. V. Oppenhiem, A. S. Willsky, and S. H. Nawab, *Signals and systems*. Prentice-Hall, 1983.